REPRESENTATIVE GROUND-MOTION ENSEMBLES FOR SEVERAL MAJOR EARTHQUAKE SCENARIOS IN NEW ZEALAND

Karim Tarbali[1] and Brendon A. Bradley[2]

SUMMARY

In this paper, representative ground motion ensembles for several major earthquake scenarios in New Zealand are developed. Cases considered include representative ground motions for the occurrence of Alpine, Hope and Porters Pass earthquakes in Christchurch city, and the occurrence of Wellington, Wairarapa and Ohariu fault ruptures in Wellington city. For each considered scenario rupture, ensembles of 20 and 7 ground motions are selected using the generalized conditional intensity measure (GCIM) approach, ensuring that the ground motion ensembles represent both the mean and distribution of ground motion intensity which such scenarios could impose. These scenario-based ground motion sets can be used to complement ground motions which are often selected in conjunction with probabilistic seismic hazard analysis, in order to understand the performance of structures for the question "what if this fault ruptures?"

INTRODUCTION

Conducting nonlinear response history analysis of structures for the purpose of seismic performance assessment requires selecting ground-motion time series which provide a hazard-consistent representation of the seismic hazard at the site. Although it is common to conduct seismic performance assessment based on the results from probabilistic seismic hazard analysis (PSHA), scenario-based assessments can also be highly informative and provide complementary insights [1].

Many methods have been proposed to select ground motions based on matching the (pseudo) acceleration response spectrum of the selected motions to a target spectrum and considering implicit causal parameters of dominant scenario ruptures (e.g. magnitude, source-to-site distance, site conditions) [2-7]. Katsanos *et al*. [8] present a detailed review of the existing ground motion selection methodologies. Typically such approaches have been considered in the context of a response spectrum obtained from the PSHA results, or a code-based response spectrum (see Oyarzo-Vera *et al* [9]) for ensembles based on NZS1170.5 standard [10] for the North Island of New Zealand). Such approaches generally have several shortcomings [11], namely: (1) ground motion severity is a function of the amplitude, frequency content, duration, and cumulative effects of the motion, which is not embodied simply in spectral acceleration ordinates; (2) ground motion ensembles should represent the full distribution of ground motion intensity and not just the mean; and (3) the ground motion ensemble should be representative of all the seismic sources which contribute to the hazard at the site. These shortcomings have been addressed through the generalized conditional intensity measure (GCIM) approach developed by Bradley [11, 12], which provides a theoretically consistent approach to obtain ground motions based on PSHA for seismic performance assessment [13]. The GCIM-based ground motion selection method has also been recently extended to select ground motions based on the results from scenario seismic hazard analysis (scenario SHA) [14, 15].

In the present study, the GCIM method is utilized to select representative ground motion ensembles for several major earthquake scenarios in New Zealand. Two sets of ensembles with 7 and 20 ground motions are selected, which can be used for scenario-based seismic performance assessment purposes (7 motions being a common number prescribed in seismic design guidelines, and the larger number necessary to adequately characterize the full distribution of seismic demand). The earthquake rupture forecast (ERF) model developed by Stirling *et al.* [16] is used to obtain the characteristics of seismic sources, and the New Zealand-specific ground motion prediction equation (GMPE) developed by Bradley [17] is used to predict spectral accelerations, peak ground acceleration, and peak ground velocity for the purposes of scenario-based seismic hazard analysis and ground-motion selection. Other ground motion intensity measures of importance in seismic hazard analysis and ground-motion selection are obtained using foreign (i.e., non-NZ-specific) GMPEs developed for active shallow crustal events. Results are first presented for rupture scenarios impacting Christchurch city then Wellington city, and finally the current challenges with ground motion selection for subduction zone ruptures are discussed.

[1] *PhD candidate, Department of Civil and Natural Resources Engineering, University of Canterbury, Christchurch, New Zealand (member)*

[2] *Senior Lecturer, Department of Civil and Natural Resources Engineering, University of Canterbury, Christchurch, New Zealand (member)*

GROUND MOTION SELECTION FOR SCENARIO RUPTURES IN CHRISTCHURCH

Dominant seismic sources

In order to identify the scenario ruptures with significant contributions to the seismic hazard at a generic location in central Christchurch city (Lat: −43.5300°; Lon: 172.6203°), PSHA was conducted using the open-source seismic-hazard-analysis software, OpenSHA [18]. The soil condition at the site is assumed to be site class D according to NZS1170.5 [10], with an inferred time-averaged 30m shear wave velocity of V_{s30} = 250 m/s. Figure 1 presents the deaggregation of the seismic hazard at this site for both peak ground acceleration (PGA) and T = 2s period spectral acceleration, SA(2.0s), for a 10% probability of exceedance in 50 years. As seen in Figure 1, the PGA seismic hazard at this generic site is mostly dominated by events with small magnitudes and small source-to-site distances associated with distributed seismicity, with similar results for SA ordinates at small vibration periods. However, as shown for the deaggregation of the SA(2.0s) hazard, events with large magnitudes and moderate-to-large source-to-site distances dominate at long vibration periods (specifically T > 1s).

Based on the scenarios with a large contribution to the seismic hazard for different periods of vibration, ground motions in Christchurch city due to ruptures of the Alpine, Hope, and Porters Pass faults are considered in this study for scenario ground-motion selection. The specific characteristics of these scenario ruptures are presented in Table 1.

Intensity measures of the considered scenario ruptures

Table 2 presents median predicted values of several intensity measures (IMs) for the rupture scenarios considered for Christchurch city. As shown, the spectral acceleration ordinates (and PGA) of the Porters Pass scenario are greater than those for scenarios with larger source-to-site distances (i.e. Alpine and Hope), especially for periods of vibration smaller than T = 2 s. Similarly, the Porter Pass rupture is predicted to produce a greater PGV compared to Alpine and Hope fault ruptures. In contrast, the Alpine fault rupture has a median predicted 5-95% Significant Duration of D_{s595}= 56.2s, which is double the Significant Duration from the Porter Pass rupture (due to a smaller magnitude and source-to-site distance in comparison to the Alpine fault rupture).

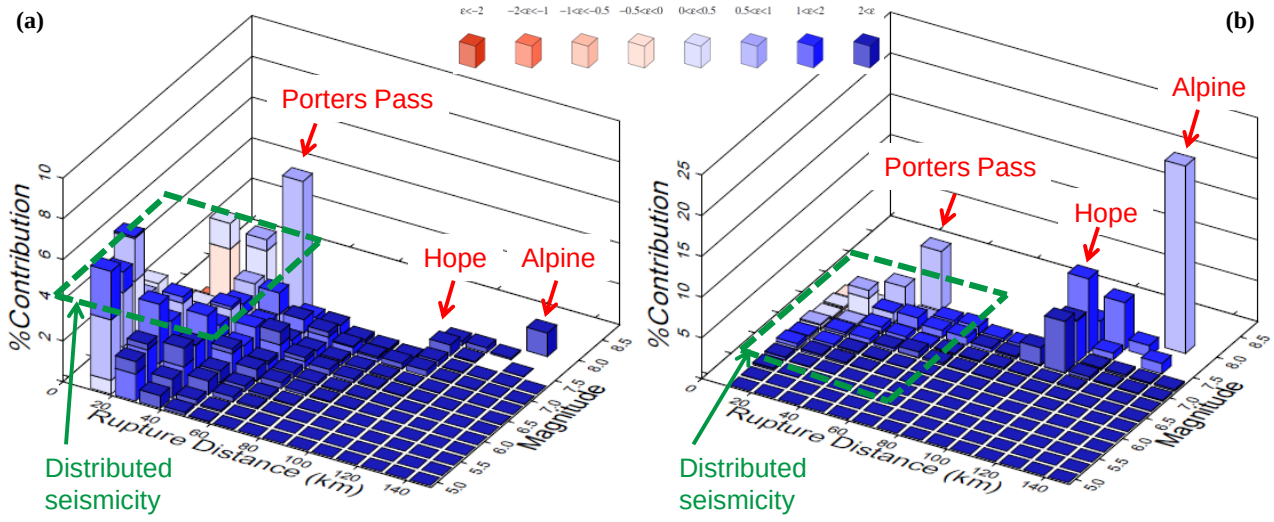

Figure 1: Deaggregation of seismic hazard in Christchurch city for a 10% probability of exceedance in 50 years: (a) PGA; and (b) SA(2.0s).

Table 1: Characteristics of the considered scenario ruptures for Christchurch city[1].

Fault	Magnitude, M_w	Source-to-site distance, R_{rup}(km)	Rupture mechanism
Alpine (Fiord-Kelly segment)	8.1	133	Strike-slip
Hope (Conway segment)	7.5	106	Strike-slip
Porters Pass	7.5	44	Strike-slip

[1]Based on the ERF of Stirling *et al.* [16].

Table 2: Median intensity measures of the considered scenario ruptures for Christchurch city.

Fault	PGA (g)	SA(0.5s) (g)	SA(1.0s) (g)	SA(2.0s) (g)	PGV (cm/s)	CAV[1] (g.s)	D_{s595}[2] (s)
Alpine (Fiord-Kelly segment)	0.07	0.13	0.11	0.07	12.1	0.9	56.2
Hope (Conway segment)	0.05	0.10	0.07	0.04	7.9	0.5	36.6
Porters Pass	0.15	0.23	0.15	0.08	18.0	0.7	27.5

[1]CAV=cumulative absolute velocity [19]; [2]D_{s595}= 5-95% Significant Duration [20].

Prior to selecting ground motions, it is important to identify the type of engineering system considered for seismic performance assessment, so that the selection process can aim to place emphasis on those IMs that are important to determine the characteristic response of the system. For instance, empirical evidence suggests that the peak inter-story drift of a building structure is strongly affected by spectral acceleration ordinates of the applied motion for periods near the first several vibration modes of the structure [e.g., 6, 21]. In contrast, for example, the response of geotechnical structures with liquefaction-susceptible soils and the collapse capacity of building structures can be considerably affected by duration and cumulative effects of ground motions [11, 22, 23]. This problem-specific issue has been addressed in the GCIM-based ground-motion selection methodology by using a weight vector in the selection algorithm to weight different ground motion IMs in record selection [12]. In order to consider different aspects of a ground motion, including amplitude, frequency content, duration, and cumulative effects, the selection process is based on distribution of multiple intensity measures for the considered rupture scenarios [12, 14].

Based on previous research [14], the considered intensity measures for the purpose of this study are: spectral acceleration for 18 vibration periods (T = 0.05, 0.075, 0.1, 0.15, 0.2, 0.25, 0.3, 0.4, 0.5, 0.75, 1.0, 1.5, 2.0, 3.0, 4.0, 5.0, 7.5, and 10.0 s), cumulative absolute velocity (CAV) [19], and Significant Durations (D_{s595} and D_{s575}) [20]. The relative importance of these intensity measures is applied by using a weight vector presented in Table 3, in which the total weight of 70% is evenly distributed across the 18 SA ordinates, and 10% weight is allocated to each of CAV, D_{s595}, and D_{s575} intensity measures. Additional intensity measures such as peak ground acceleration (PGA); peak ground velocity (PGV); acceleration spectrum intensity (ASI) [24]; spectrum intensity (SI) [25]; and displacement spectrum intensity (DSI) [26] were also considered. Although considering various intensity measures can result in motions with a proper representation for different aspects of ground motions (i.e., amplitude, frequency content, duration, and cumulative effects) for a given scenario rupture, based on the results presented by Tarbali and Bradley [14], considering SA ordinates, CAV, and Significant Duration intensity measures (i.e., D_{s595} and D_{s575}) can fairly represent these aspects. Therefore, only these intensity measures are given non-zero weights in the implemented weight vector (Table 3). Further details on the impact of weight vector selection are discussed at length in Tarbali and Bradley [14].

Selected 20 ground motions for scenario ruptures in Christchurch

For each of the considered scenarios, 20 ground-motion time series are selected from the NGA database of strong ground motions from active shallow crustal earthquakes [27]. As discussed by Tarbali and Bradley [14], limiting the available database of ground motions to those motions with implicit casual parameters (e.g., magnitude, source-to-site distance, site condition) similar to the characteristics of the considered scenario rupture can result in motions with an appropriate representation for the causal parameters of the scenario, along with the explicit intensity measures of motion. In this regard, for each scenario considered, the NGA database is limited based on the bounds presented in Table 4. As seen in this table, the prospective ground motions are limited to those motions one unit of magnitude greater and smaller than the corresponding rupture scenario magnitude, and the source-to-site distances of the motions (R_{rup}) are bounded to 0.5 to 1.5 times the scenario R_{rup}. The site condition of the prospective motions is limited to site class D (deep or soft soils) and E (very soft soils) [10], using V_{s30} values less than 400 m/s. The implemented bounds on these causal parameters are wide in order to avoid an unreasonably small number of prospective ground motions for the considered scenario ruptures. However, it is re-iterated that the selected ground motions are not based on specific causal parameters once this first screening criteria has been applied.

It should also be noted that the motions in the NGA database have been processed to be directly used in seismic response analyses and are accessible at http://peer.berkeley.edu/nga/. The ground motions selected in this study are presented in Appendix A and B of this paper and can also be downloaded from https://sites.google.com/site/brendonabradley/research/ground-motion-selection.

In order to illustrate the properties of the selected motions, Figure 2 presents the median, 16th and 84th percentiles, and the individual acceleration response spectra of the selected motions (which have been amplitude scaled), along with the predicted median target spectrum and the target 16th and 84th percentile spectra for the considered rupture scenarios. In addition, Figure 2d presents the cumulative distribution of 5-95% Significant Duration, D_{s595}, for the considered rupture scenarios and the corresponding target distribution.

Table 3: Weight vector considered for ground-motion selection.

SA	CAV	D_{s575}	D_{s595}
0.7[1]	0.1	0.1	0.1

[1]Evenly distributed to 18 SA ordinates between T=0-10s, i.e., each SA ordinate has a weight of 0.7/18.

Table 4: Bounds on the implicit causal parameters of the prospective ground motions for the considered scenario ruptures for Christchurch city.

Faults	Magnitude, M_w	Source-to-site distance, R_{rup} (km)	Site condition, V_{s30} (m/s)
Alpine (Fiord-Kelly segment)	$7.1 \le M_w \le 9.1$	$66 \le R_{rup} \le 198$	$V_{s30} \le 400$
Hope (Conway segment)	$6.5 \le M_w \le 8.5$	$53 \le R_{rup} \le 159$	$V_{s30} \le 400$
Porters Pass	$6.5 \le M_w \le 8.5$	$22 \le R_{rup} \le 66$	$V_{s30} \le 400$

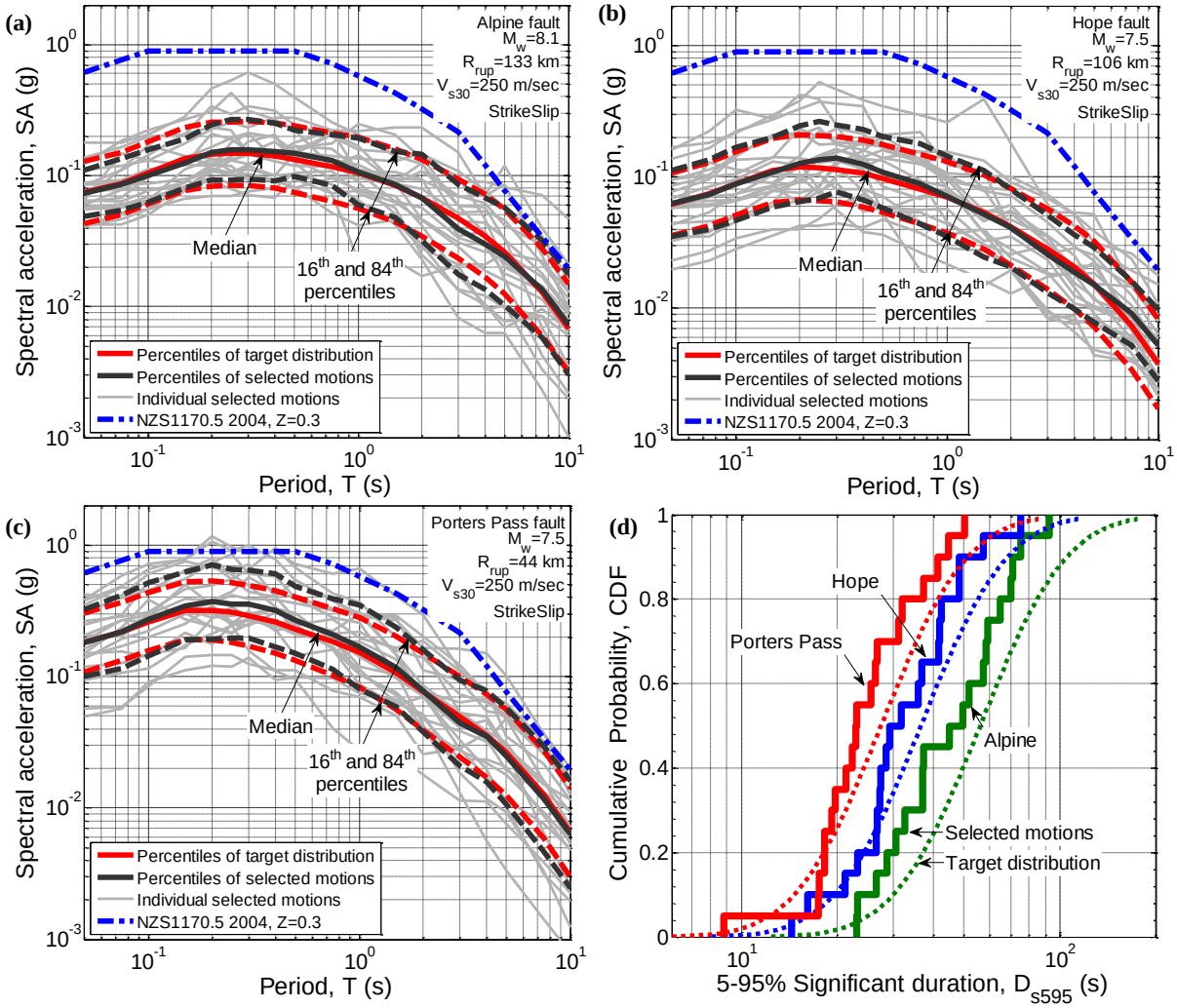

Figure 2: SA ordinates of the selected ground motions and the corresponding median, 16th, and 84th percentile spectra representing: (a) Alpine; (b) Hope; (c) Porters Pass scenario ruptures; and (d) cumulative distribution of 5-95% Significant Duration and the corresponding target distribution for the considered scenario ruptures.

Based on the presented results, it can be seen that the distribution of SA ordinates of the selected motions provides an unbiased representation of the predicted target distribution (i.e., 16th, 50th, and 86th percentiles of the selected motions conform to the predicted target distribution). Also, the distribution of D_{s595} (Figure 2d), along with CAV and 5-75% Significant Duration, D_{s575}, (although not presented here for brevity) of the selected motions corresponds well to the target distribution of the scenario ruptures.

As seen in Figure 2, the predicted median scenario spectrum, the median spectrum of the selected motions, and the individual acceleration response spectrum of majority of the selected motions for the corresponding scenario ruptures are below the elastic site spectra presented in NZS1170.5 [10] for Christchurch (Z= 0.3; shown here for reference only). In addition, as presented in Figure 2d, the M_w8.1 rupture of the Alpine fault and M_w7.5 rupture of the Hope fault (both with large source-to-site distances) will produce motions with long Significant Durations, whereas the M_w7.5 rupture of the Porter Pass fault (with a smaller source-to-site distance) will result in motions with shorter Significant Durations. The large differences in Significant Duration of the considered rupture scenarios and the considerable effect of duration on seismic response of engineering systems [11, 22, 23] illustrates the importance of considering this intensity measure when selecting ground motions for seismic response analysis.

Considering the fact that the implicit causal parameters of ground motions, such as magnitude, source-to-site distance, and site condition are not explicitly considered in the GCIM-based ground-motion selection methodology [12, 14], it is worthwhile examining the distribution of these parameters for the selected motions with respect to each scenario rupture. As illustrated in Figure 3, the selected motions for the Hope fault rupture are well distributed with respect to the scenario magnitude (i.e. the 16th to 84th percentile range of M_w encompass the scenario). This is also generally the case for the Porters Pass fault rupture. In contrast, the selected motions for the Alpine fault rupture have a lower magnitude distribution than the scenario itself. This is caused by the paucity of recorded ground motions with magnitudes larger than M_w7.5-8.0, in contrast to a relative abundance in the recorded motions from events with smaller magnitudes. This is illustrated in Figure 3d, which depicts the M_w-R_{rup} distribution of the motions in the NGA database [27] and the motions that are available for the considered rupture scenarios for Christchurch city based on the bounds presented in Table 4. As seen in Figure 3d, a small portion of the total database of motions is available for the Alpine fault rupture relative to the other two scenarios. Figure 3a-c also illustrates that the selected ground motions can properly represent the scenario source-to-site distance for all three of the considered scenario ruptures, with the mean R_{rup} very close to the target scenario R_{rup}.

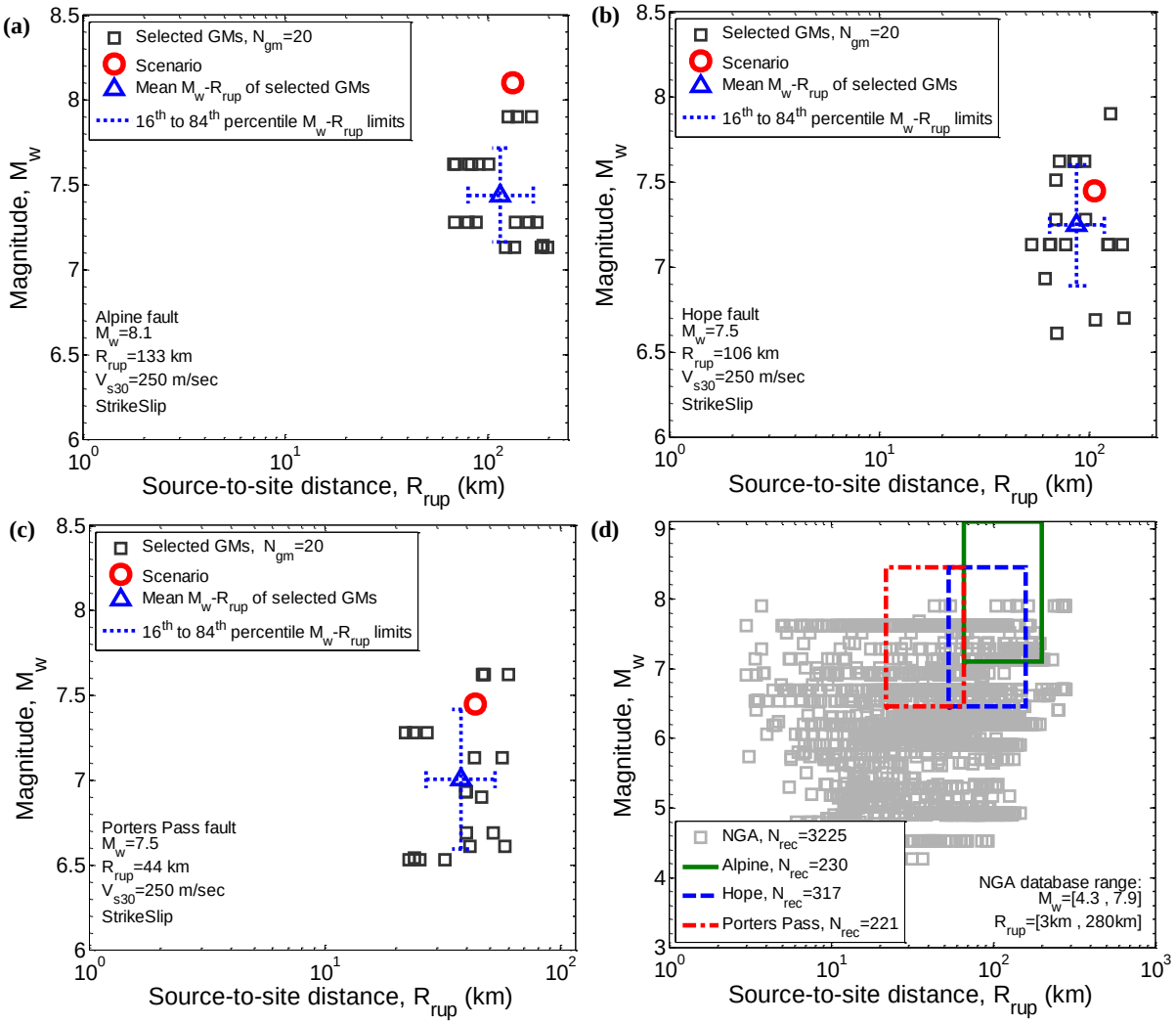

Figure 3: ***Magnitude-distance distribution of the selected motions representing: (a) Alpine; (b) Hope; (c) Porters Pass scenario ruptures; (d) available ground motions in the database based on the bounds applied on the casual parameters of prospective ground motions.***

Figure 4a-c presents the V_{s30}-R_{rup} distribution of the selected motions representing the considered scenarios for Christchurch city. As shown, the selected motions encompass the scenario within the 16th to 84th percentile bound. Also, the median V_{s30} of the selected motions is similar to the V_{s30} of the considered generic site. As discussed in [14], imposing bounds on magnitude, source-to-site distance, and site condition of prospective ground motion results in motions with a proper representation for these causal parameters, which is illustrated in Figure 3a-c and Figure 4a-c for the considered scenario ruptures for Christchurch city. In addition to the distributions of the causal parameters (M_w, R_{rup} V_{s30}), the amplitude scale factor, *SF*, applied on the selected motions can be used to check the quality of the obtained ensemble of ground motions. Figure 4d presents the amplitude scale factor of the selected motions for the considered rupture scenarios for Christchurch city. It is noted that the amplitude scale factors are not constrained by the ground motion selection methodology, but are a by-product of representing the target IMs in an unbiased fashion based on the bounded prospective ground motions. As seen in this figure, all of the amplitude scale factors for the Hope fault rupture and 90% of the amplitude scale factors for the rupture of Alpine and Porter Pass faults are in the range of 0.3 to 3.0. Similar ranges are often recommended as scaling limits in seismic design standards [e.g., 28, 10]. It should be noted that, as discussed by Tarbali and Bradley [14], having bounds on the implicit causal parameters of the prospective ground motions results in selecting motions with smaller amplitude scaling factors. This is due to the fact that by limiting the available motions to those with causal parameters similar to the scenario characteristics, small changes in the amplitude of the motions are required to represent the distribution of the explicit intensity measures of motion.

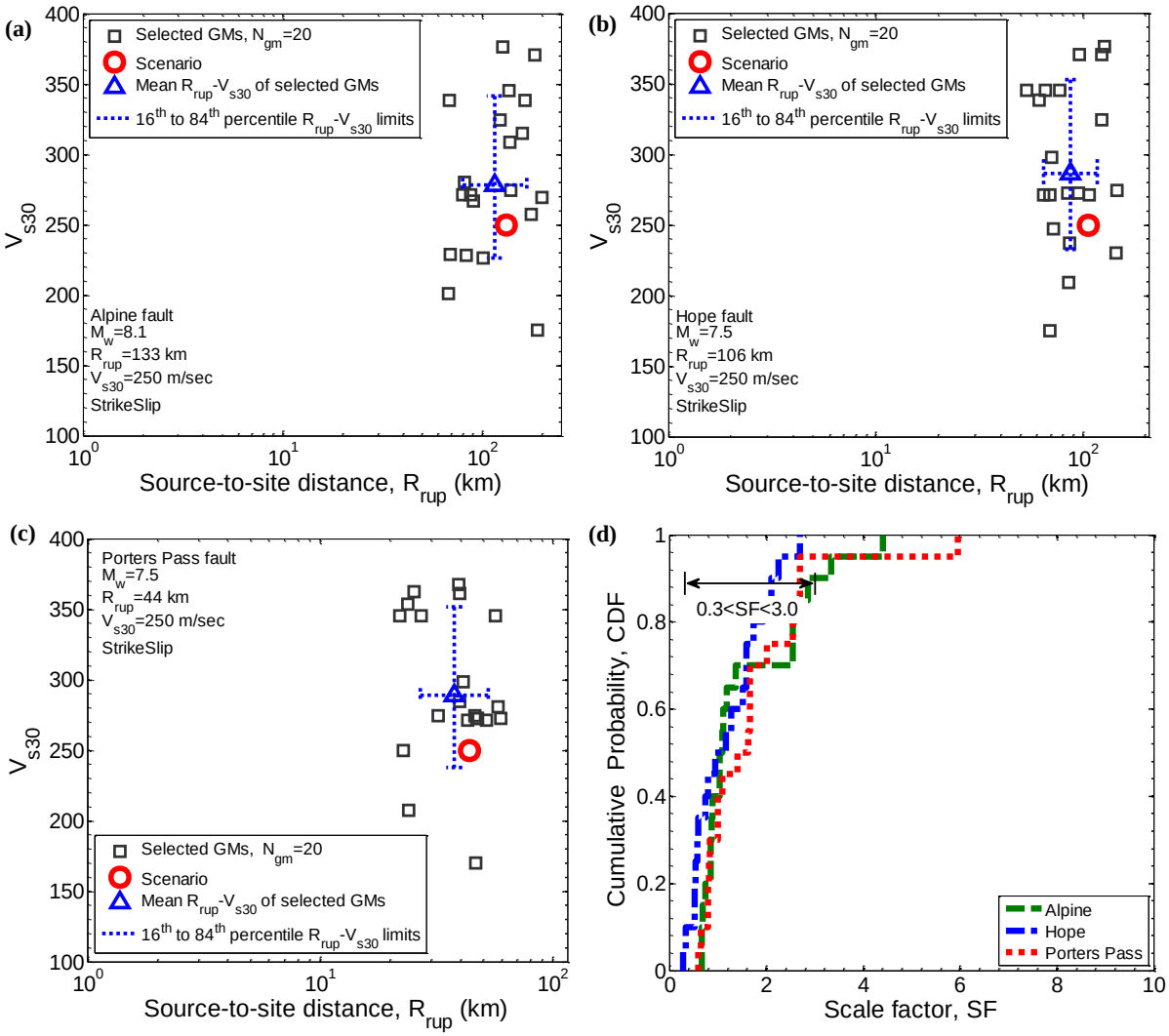

Figure 4: V_{s30} -R_{rup} distribution of the selected ground motions, representing: (a) Alpine; (b) Hope; and (c) Porters Pass scenario ruptures, and (d) cumulative distribution of the amplitude scale factor of the selected motions.

It is important to note that there is a trade-off when selecting motions to achieve an unbiased distribution of the predicted intensity measures (SA, D_{s595} etc.); magnitude-distance distribution (or other implicit causal parameters); and amplitude scale factors. While ideally the selected motions would have the appropriate representation of implicit causal parameters and amplitude scale factors near 1.0, an emphasis in ground motion selection should be placed on the distribution of the explicit intensity measures of the ground motion (SA, D_{s595} etc.) rather than the implicit causal parameters, as elaborated on by Bradley [12] and Tarbali and Bradley [14].

A subset of 7 ground motions from the selected 20 motions

A subset of 7 ground motions from the selected 20 motions are also tabulated in Appendix B, which can be used in code-based analyses to assess the design or retrofit of the engineering systems against the occurrence of the considered rupture scenarios. Figure 5, as an example, illustrates the SA ordinates, cumulative distribution of 5-95% Significant Duration, M_w-R_{rup} and V_{s30}-R_{rup} distributions of the subset of 7 motions representing the Alpine fault scenario rupture.

As seen in Figure 5, the selected 7 ground motions provide an unbiased representation of the predicted IMs of the motions for the scenario rupture. Considering the distribution of the causal parameters of the 20 motions, the V_{s30} and R_{rup} of the subset of 7 motions have an appropriate representation of the scenario characteristics. It is important to note that the individual amplitude scale factors applied on these 7 motions, in order to collectively represent the predicted distribution of the considered IMs, are slightly different than those applied on the same motions when they were selected in a set with 20 motions. As presented in Appendix B, all of the amplitude scale factors applied on the subset of 7 motions are within the range of 0.3 to 3.0.

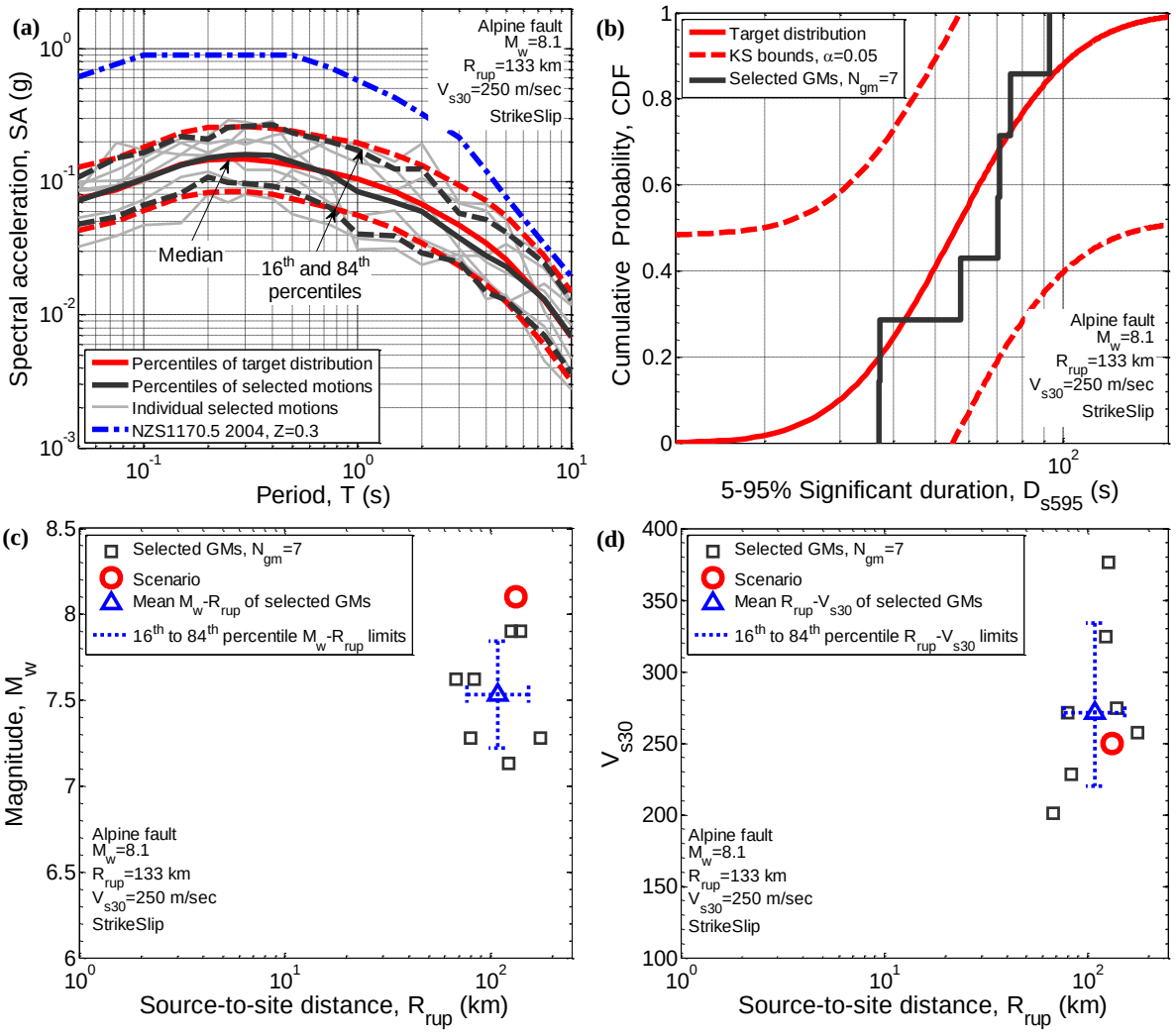

Figure 5: Properties of the subset of 7 ground motions representing the Alpine fault scenario rupture: (a) SA ordinates; (b) cumulative distribution of 5-95% Significant Duration; (c) M_w-R_{rup} distribution; and (d) V_{s30}-R_{rup} distribution.

GROUND MOTION SELECTION FOR SCENARIO RUPTURES IN WELLINGTON

Dominant seismic sources

PSHA has been conducted for a generic location in central Wellington city (Lat: −41.2889°; Lon: 174.7772°) for a site class D soil (NZS1170.5 2004) with V_{s30} = 250 m/s. Figure 6 illustrates the seismic hazard deaggregation for PGA and SA(2.0s) for a 10% probability of exceedance in 50 years. Based on the obtained results for deaggregation of the seismic hazard, it is observed that the seismic hazard at this generic location in Wellington city is mostly dominated by events with large magnitudes and very small source-to-site distances. By identifying the scenarios with large contributions to the seismic hazard, ruptures of the Wellington, Wairarapa, and Ohariu faults are considered in this study for scenario ground-motion selection. Characteristics of these scenario ruptures are presented in Table 4.

It is important to note that the presented deaggregation results illustrate the contribution of a M_w8.6 rupture of the Hikurangi subduction zone ("Wellington Max segment") approximately 20 km from Wellington city. The current issues related to robustly selecting ground motions to represent subduction zone earthquakes are presented later in this paper, and therefore attention here has been limited to selecting ground motions to represent active shallow-crustal ruptures.

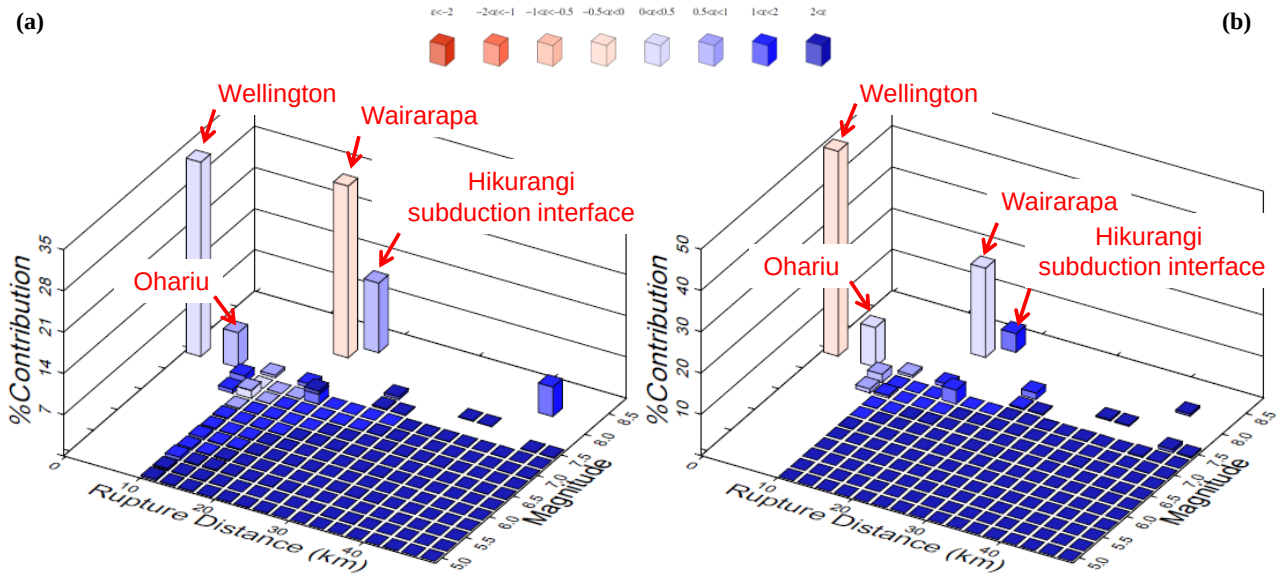

Figure 6: Deaggregation of seismic hazard in Wellington city for a 10% probability of exceedance in 50 years: (a) PGA; and (b) SA(2.0s).

Table 5: Characteristics of the considered scenario ruptures for Wellington city[1].

Fault	Magnitude, M_w	Source-to-site distance, R_{rup} (km)	Rupture mechanism
Wellington (Well-Hutt Valley segment)	7.5	1.0	Strike-slip
Wairarapa (Nicholson segment)	8.2	17.0	Strike-slip
Ohariu (South segment)	7.4	6.0	Strike-slip

[1]Based on the ERF of Stirling *et al.* [16].

Table 6. Median intensity measures of the considered scenario ruptures for Wellington city.

Fault	PGA (g)	SA(0.5s) (g)	SA(1.0s) (g)	SA(2.0s) (g)	PGV(cm/s)	CAV(g.s)	Ds595 (s)
Wellington (Well-Hutt Valley segment)	0.6	1.0	0.9	0.6	104.7	2.0	24.0
Wairarapa (Nicholson segment)	0.7	1.1	0.8	0.4	74.7	2.0	41.5
Ohariu (South segment)	0.5	0.7	0.6	0.4	70.0	2.1	21.0

Intensity measures of the considered scenario ruptures

Table 6 presents the median intensity measures for the scenario ruptures considered for Wellington city. As presented, the Wellington fault with a large magnitude and very small R_{rup}, and the Wairarapa fault with a very large magnitude and small R_{rup} have close median SA ordinates. In addition, the Wellington rupture results in a greater PGV compared to the Wairarapa and Ohariu ruptures, because of the very small source-to-site distance from this fault to the site. Finally, because of the large magnitude of the rupture in the Wairarapa fault (i.e., M_w 8.2), the median predicted ground motion Significant Duration (i.e., median D_{s595}) is considerably greater than that for the other two ruptures.

Selected 20 ground motions for scenario ruptures in Wellington

Similar to the Christchurch scenarios previously discussed, ensembles of 20 ground motions were selected for each of the three considered ruptures for Wellington city, using the GCIM-based ground-motion selection method. Table 7 presents the bounds applied on the implicit causal parameters of the prospective ground motions for the three considered scenario ruptures. Due to the short source-site distance of the three considered scenarios, R_{rup} of the prospective ground motions are bounded to values less than 30 km. The weight vector presented in Table 3 is also implemented here for the Wellington city cases.

Figure 7a-c presents the median, 16th, and 84th percentiles and the individual (amplitude scaled) acceleration response spectrum of the selected motions, along with the predicted median, 16th, and 84th percentile target spectra for the considered scenario ruptures for Wellington city. As shown in Figure 7a-b, the predicted median scenario spectrum, and the median spectrum of the selected motions for rupture of the Wellington fault (which has the highest contribution to the seismic hazard at the site) and Wairarapa fault are very close to the Z = 0.4 elastic code spectra of NZS1170.5 [10] at medium to long periods of vibration (provided here for comparison only).

Table 7: Bounds on the implicit causal parameters of the prospective ground motions for the considered scenario ruptures for Wellington city.

Faults	Magnitude, M_w	Source-to-site distance, R_{rup} (km)	Site condition, V_{s30} (m/s)
Wellington (Well-Hutt Valley segment)	$6.5 \leq M_w \leq 8.5$	$R_{rup} \leq 30$	$V_{s30} \leq 400$
Wairarapa (Nicholson segment)	$7.2 \leq M_w \leq 9.2$	$R_{rup} \leq 30$	$V_{s30} \leq 400$
Ohariu (South segment)	$6.4 \leq M_w \leq 8.4$	$R_{rup} \leq 30$	$V_{s30} \leq 400$

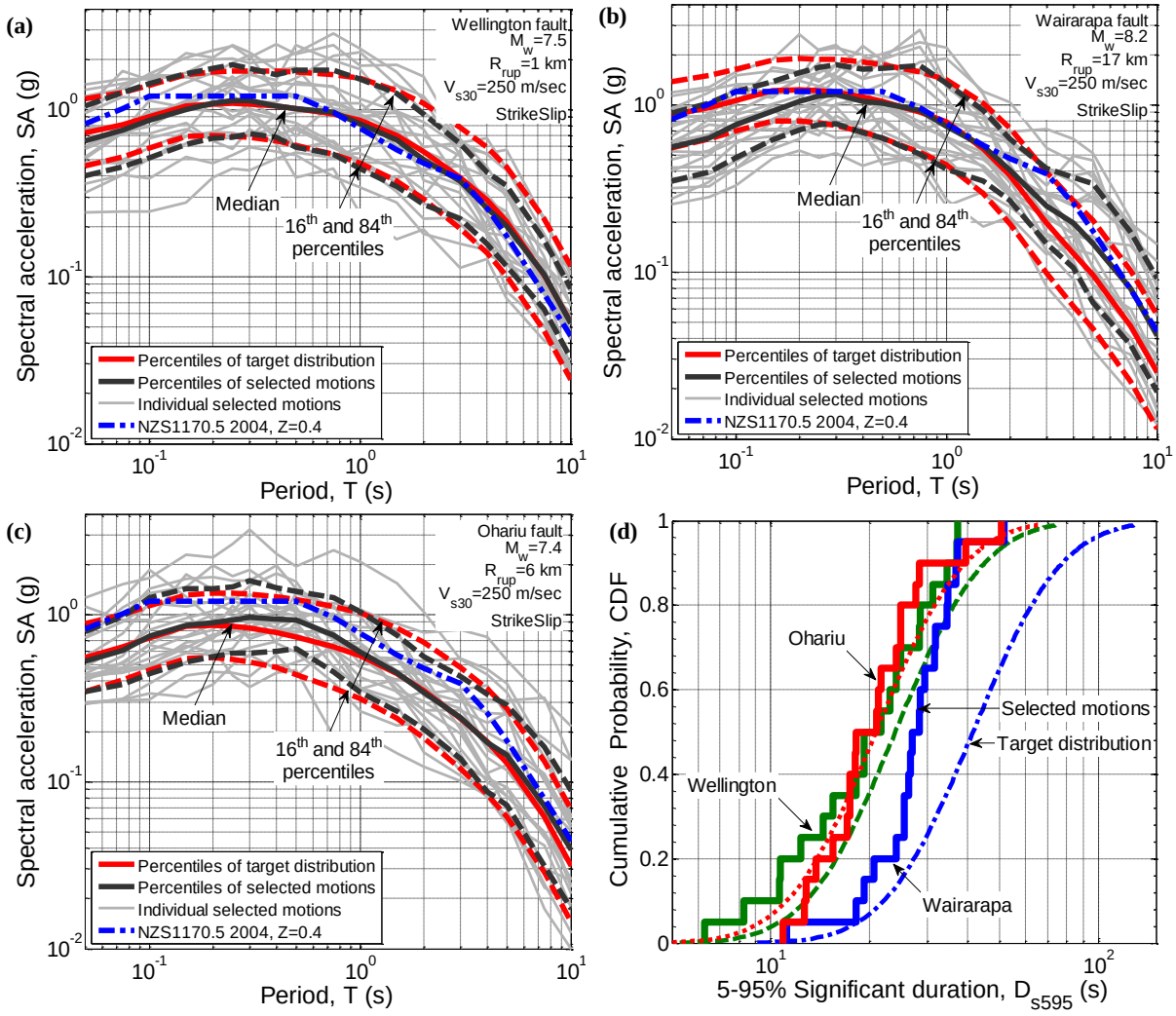

Figure 7: SA ordinates of the selected motions and the corresponding median, 16th, and 84th percentile spectra representing: (a) Wellington; (b) Wairarapa; (c) Ohariu scenario ruptures; and (d) cumulative distribution of 5-95% Significant Duration and the corresponding target distribution for the considered scenario ruptures.

As presented in Figure 7a-c, the selected ground motions provide an unbiased representation of the SA ordinates for Wellington and Ohariu fault ruptures, for the whole range of vibration periods (i.e., T = 0.05 s-10.0 s). However for the Wairarapa fault rupture, the selected motions deviate from the target distribution for short (i.e., T < 0.2) and long (i.e., T > 4.0) vibration period ranges. Also, based on the presented cumulative distribution of the 5-95% Significant Duration of the selected ground motions and the corresponding target distribution in Figure 7d, it can be seen that the selected motions can properly represent the 5-95% Significant Duration for the Wellington and Ohariu fault ruptures. However, there is a deviation from the target distribution for 5-95% for the Wairarapa fault rupture. When considering the resulting ground motions selected for the Wairarapa rupture scenario (Figure 7b and Figure 7d), it is important to note that in comparing the selected motions with the 'target' we are implicitly assuming that the target is itself correct. While this is generally a reasonable assumption, in the case of rupture scenarios with very large magnitudes, (i.e., M_w8.2 for Wairarapa), the GMPE utilized to calculate the target distribution is weakly constrained for such large events. Therefore, the 'target' may itself be inherently biased, but future research is needed to more appropriately constrain such an assertion.

Figure 8 provides a comparison of the magnitude-distance distribution of the selected motions with respect to magnitude-distance pair of the corresponding scenarios for Wellington city. In the case of the Wellington and Ohariu fault ruptures, it can be seen that the magnitude distribution of the selected

motions fairly corresponds to the rupture magnitude, while the magnitudes of the selected motions for the Wairarapa rupture fall below the scenario magnitude. In terms of source-to-site distances it can be seen that the ground motions selected for the Wairarapa fault rupture corresponds well to the scenario source-to-site distance, with a mean R_{rup} very close to the scenario R_{rup}. However, the source-to-site distances of the selected motions for the Wellington and Ohariu fault ruptures are notably larger than those representative of these scenarios. Clearly, these biases are related to the paucity of the motions recorded from large magnitude events with short source-to-site distances. Figure 8d illustrates the M_w-R_{rup} distribution of the motions in the NGA database [27] and the ones that are available for each rupture scenario for Wellington city based on the bounds presented in Table 7. As shown, there are few motions with implicit causal parameters close to the characteristics of the Wairarapa fault rupture relative to the other two scenarios.

As already noted, it is important to remember that ground-motion selection requires a trade-off between the intensity measure values of the ground motions themselves, and implicit causal parameters such as M_w, R_{rup}, V_{s30}, etc. Because it is known that there is little variation of ground motion properties in the immediate near-field (i.e., R_{rup} = 0-10km) region, then the distance biases shown in Figure 8 for the Wellington and Ohariu fault ruptures (with R_{rup} values of 1.0 and 6.0 km, respectively) are not considered significant.

Figure 9a-c presents V_{s30}-R_{rup} distribution of the selected ground motions representing the considered scenarios for Wellington city. As shown, the V_{s30} values of the selected motions for the Wellington and Ohariu fault ruptures correspond well to the considered site condition. Also, most of the selected motions for the Wairarapa fault rupture have V_{s30} values which are mostly similar to characteristics of a site class D soil (NZS1170.5 [10]).

As presented in Figure 9d, the amplitude scale factor of the selected motions are mostly large values, compared to the results presented in Figure 4d for Christchurch city, with approximately 80% of them for Wellington and Wairarapa fault ruptures and 70% of them for Ohariu fault rupture in the *SF*= 0.3-3.0 range. As discussed by Tarbali and Bradley [14], selecting ground motions for scenarios like those encountered in Wellington city (with short source-to-site distances and large magnitudes) often requires scaling the existing motions using larger scale factors, as there is a shortage of motions recorded during such events in the existing strong ground motion database [27] with adequate intensity measure properties and recorded at appropriate site classes.

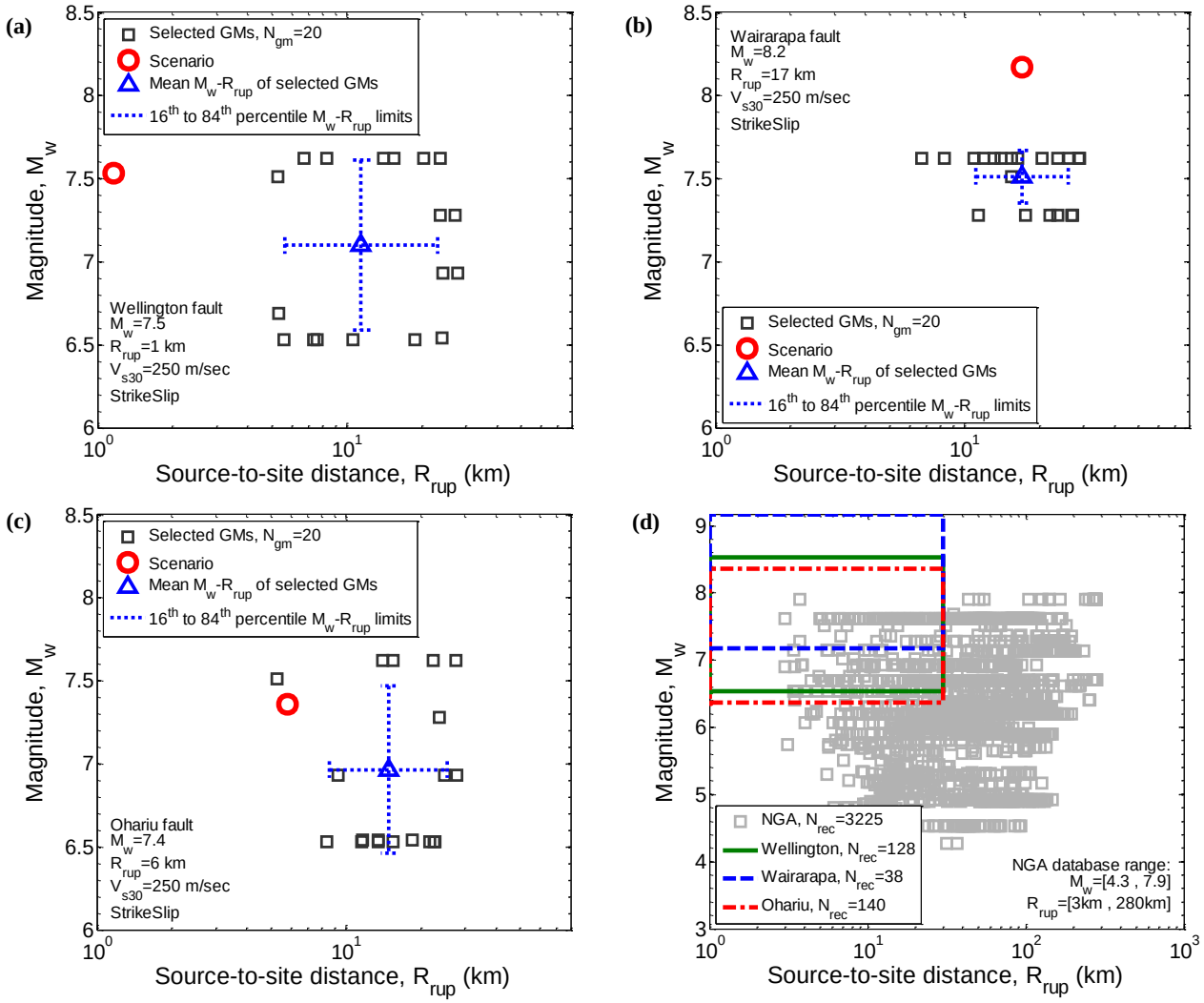

***Figure 8:** Magnitude-distance distribution of the selected motions representing: (a) Wellington; (b) Wairarapa; (c) Ohariu scenario ruptures; (d) available ground motions in the database based on the bounds applied on the casual parameters of prospective ground motions.*

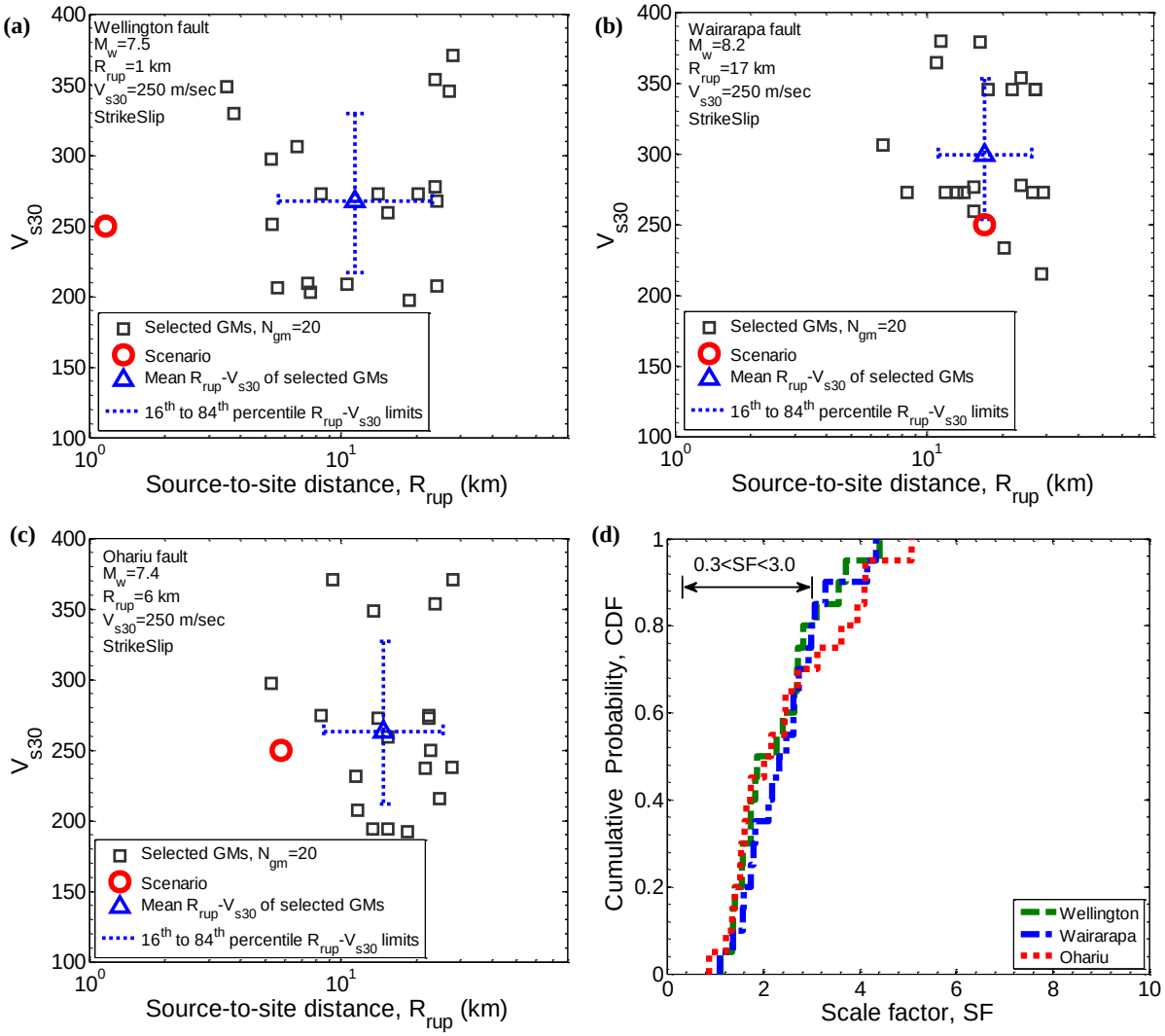

Figure 9: V_{s30}-R_{rup} distribution of the selected ground motions, representing: (a) Wellington; (b) Wairarapa; and (c) Ohariu scenario ruptures, and (d) cumulative distribution of the amplitude scale factor of the selected motions

A subset of 7 ground motions from the selected 20 motions

A subset of 7 ground motions from the selected 20 motions are also tabulated in Appendix B to represent the considered scenario ruptures in Wellington city. Figure 10 illustrates the SA ordinates, cumulative distribution of 5-95% Significant Duration, M_w-R_{rup} and V_{s30}-R_{rup} distributions of the subset of 7 motions representing the Wellington fault scenario rupture. As seen in this figure, the selected 7 motions provide an unbiased representation of the predicted distribution of the considered intensity measures. However, the issues associated with representativeness of the causal parameters of the 20 motions elaborated earlier are present in the subset of 7 motions.

SELECTING REPRESENTATIVE GROUND MOTIONS FOR SUBDUCTION ZONE EVENTS

The ground motions selected in this study are aimed to represent major active shallow crustal rupture scenarios in Christchurch and Wellington cities. However, the occurrence of major subduction zone earthquakes (both interface and slab) should also be considered in ground-motion selection for regions prone to this type of earthquakes, such as Wellington. As noted, in the presented deaggregation results for Wellington, the occurrence of a M_w8.6 rupture of the Hikurangi subduction interface (Wellington Max segment) within approximately 20 km distance of Wellington city contributes significantly to the seismic hazard. At present, routine ground motion selection for subduction zone events is hindered by a lack of: (1) a comprehensive database of strong ground motions recorded from subduction zone events; and (2) appropriate subduction zone GMPEs and correlation equations for various ground-motions intensity measures. Such efforts are topics of on-going research among the authors as well as many others in the research community.

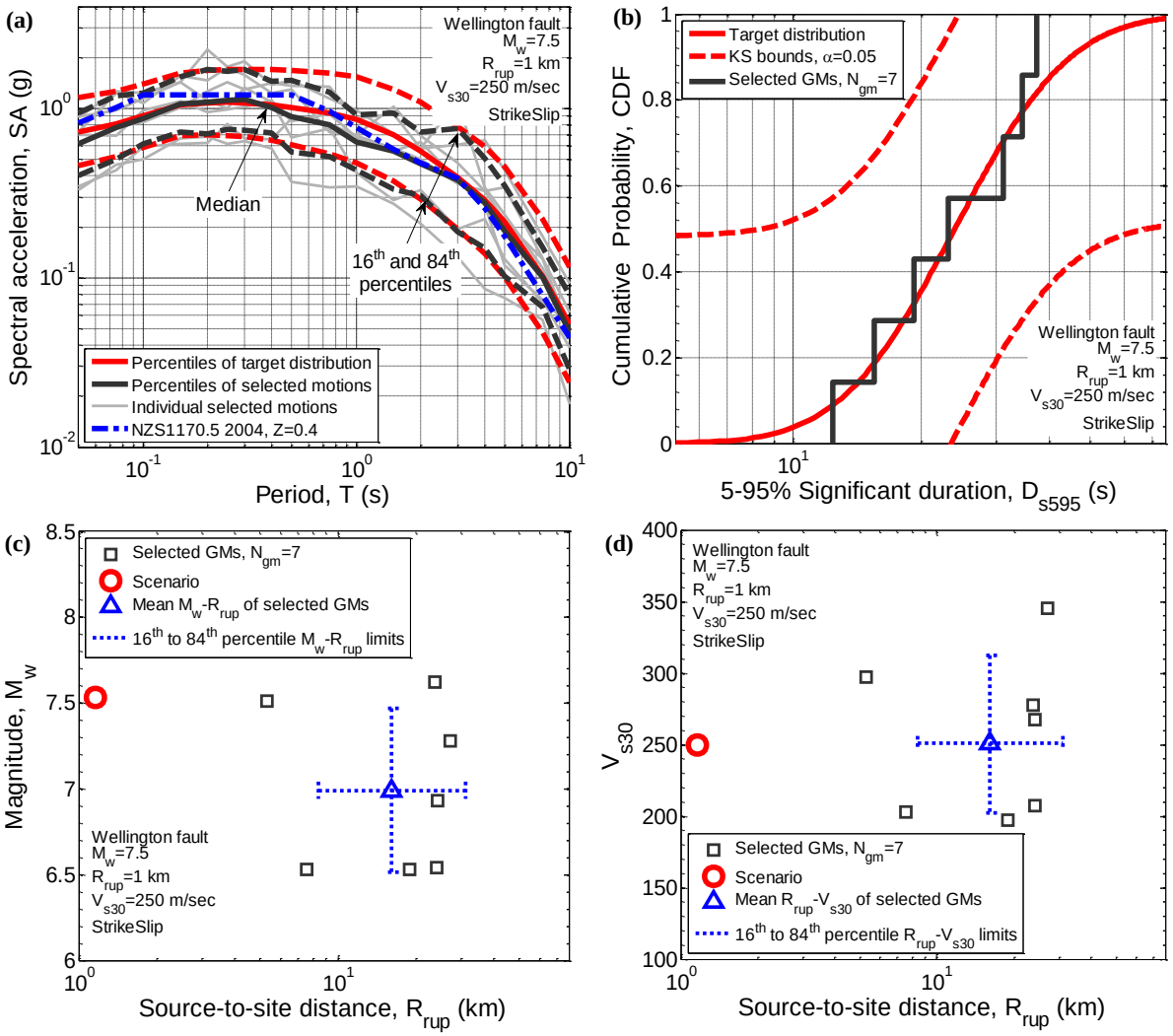

Figure 10: Properties of the subset of 7ground motions representing the Wellington fault scenario rupture: (a) SA ordinates; (b) cumulative distribution of 5-95% Significant Duration; (c) M_w-R_{rup} distribution; and (d) V_{s30}-R_{rup} distribution.

CONCLUSION

This paper demonstrates the selection of ground motions to represent several major earthquake scenarios in New Zealand, using the generalized conditional intensity measure (GCIM) approach. Six different rupture scenarios were considered that pose a significant seismic hazard in Christchurch city (Alpine, Hope and Porters Pass ruptures) and Wellington city (Wellington, Ohariu, and Wairarapa ruptures). For each rupture scenario considered, sets of 20 ground motions were selected to represent the predicted distribution of various intensity measures (spectral accelerations, Significant Duration etc.). Subsets of 7 motions from these 20 ground motions were also tabulated and can be utilized for standard code-based seismic response analyses. A paucity of recorded motions from events with large magnitudes and short source-to-site distances in existing strong ground motion databases impedes selecting motions for large magnitude small source-to-site distance rupture scenarios and also consequently requires the use of large amplitude scale factors to scale available motions. However, it should be remembered that implicit causal parameters, such as magnitude and source-to-site distance, are of secondary importance when compared to explicit measures of intensity of ground motion (spectral accelerations, Significant Duration etc.).

ACKNOWLEDGMENTS

Financial support of the University of Canterbury and New Zealand Earthquake Commission (EQC) are greatly appreciated.

REFERENCES

1 Bommer, J.J. (2002) "Deterministic vs. probabilistic seismic hazard assessment: an exaggerated and obstructive dichotomy". *Journal of Earthquake Engineering*. **6**(spec01): p. 43-73.

2 Baker, J.W. (2010) "Conditional mean spectrum: Tool for ground-motion selection". *Journal of Structural Engineering*. **137**(3): p. 322-331.

3 Bommer, J.J. and Acevedo, A.B. (2004) "The use of real earthquake accelerograms as input to dynamic analysis". *Journal of Earthquake Engineering*. **8**(spec01): p. 43-91.

4 Jayaram, N., Lin, T. and Baker, J.W. (2011) "A computationally efficient ground-motion selection algorithm for matching a target response spectrum mean and variance". *Earthquake Spectra*. **27**(3): p. 797-815.

5 Kottke, A. and Rathje, E.M. (2008) "A semi-automated procedure for selecting and scaling recorded earthquake motions for dynamic analysis". *Earthquake Spectra*. **24**(4): p. 911-932.

6 Shome, N., Cornell, C.A., Bazzurro, P. and Carballo, J.E. (1998) "Earthquakes, records, and nonlinear responses". *Earthquake Spectra*. **14**(3): p. 469-500.

7 Wang, G. (2011) "A ground motion selection and modification method capturing response spectrum characteristics and variability of scenario earthquakes". *Soil Dynamics and Earthquake Engineering*. **31**(4): p. 611-625.

8 Katsanos, E.I., Sextos, A.G. and Manolis, G.D. (2010) "Selection of earthquake ground motion records: A state-of-the-art review from a structural engineering perspective". *Soil Dynamics and Earthquake Engineering*. **30**(4): p. 157-169.

9 Oyarzo-Vera, C.A., McVerry, G.H. and Ingham, J.M. (2012) "Seismic zonation and default suite of ground-motion records for time-history analysis in the North Island of New Zealand". *Earthquake Spectra*. **28**(2): p. 667-688.

10 NZS1170.5, "NZS1170.5:2004, Structural design actions. Part 5: Earthquake actions - New Zealand", 2004, Standards New Zealand: Wellington, NZ.

11 Bradley, B.A. (2010) "A generalized conditional intensity measure approach and holistic ground-motion selection". *Earthquake Engineering & Structural Dynamics*. **39**(12): p. 1321-1342.

12 Bradley, B.A. (2012) "A ground motion selection algorithm based on the generalized conditional intensity measure approach". *Soil Dynamics and Earthquake Engineering*. **40**: p. 48-61.

13 Bradley, B.A. (2012) "The seismic demand hazard and importance of the conditioning intensity measure". *Earthquake Engineering & Structural Dynamics*. **41**(11): p. 1417-1437.

14 Tarbali, K. and Bradley, B.A. "Ground-motion selection for scenario ruptures using the generalized conditional intensity measure (GCIM) approach and its application for several major earthquake scenarios in New Zealand. University of Canterbury Research Report No. 2014-03", 2014: Department of Civil and Natural Resources Engineering, University of Canterbury, New Zealand. p. 92.

15 Tarbali, K. and Bradley, B.A. (2014) "Scenario-based ground-motion selection using the generalized conditional intensity measure (GCIM) approach". in *Proceedings of the 10th National Conference in Earthquake Engineering*. Anchorage, AK: Earthquake Engineering Research Institute.

16 Stirling, M., McVerry, G., Gerstenberger, M., Litchfield, N., Van Dissen, R., Berryman, K., Barnes, P., Wallace, L., Villamor, P. and Langridge, R. (2012) "National seismic hazard model for New Zealand: 2010 update". *Bulletin of the Seismological Society of America*. **102**(4): p. 1514-1542.

17 Bradley, B.A. (2013) "A New Zealand-Specific Pseudospectral Acceleration Ground-Motion Prediction Equation for Active Shallow Crustal Earthquakes Based on Foreign Models". *Bulletin of the Seismological Society of America*. **103**(3): p. 1801-1822.

18 Field, E.H.,. Jordan, T.H. and Cornell, C.A. (2003) "OpenSHA: A developing community-modeling environment for seismic hazard analysis". *Seismological Research Letters*. **74**(4): p. 406-419.

19 Campbell, K.W. and Bozorgnia, Y. (2010) "A ground motion prediction equation for the horizontal component of cumulative absolute velocity (CAV) based on the PEER-NGA strong motion database". *Earthquake Spectra*. **26**(3): p. 635-650.

20 Bommer, J.J., Stafford, P.J. and Alarcón, J.E. (2009) "Empirical equations for the prediction of the significant, bracketed, and uniform duration of earthquake ground motion". *Bulletin of the Seismological Society of America*. **99**(6): p. 3217-3233.

21 Tothong, P. and Cornell, C.A., "Probabilistic seismic demand analysis using advanced ground motion intensity measures, attenuation relationships and near-fault effects. John A. Blume Earthquake Engineering Center, Department of Civil and Environmental Engineering, Stanford University, Stanford, CA", 2007.

22 Bradley, B.A., Araki, K., Ishii, T. and Saitoh, K. (2013) "Effect of lattice-shaped ground improvement geometry on seismic response of liquefiable soil deposits via 3-D seismic effective stress analysis". *Soil Dynamics and Earthquake Engineering*. **48**: p. 35-47.

23 Villaverde, R. (2007) "Methods to assess the seismic collapse capacity of building structures: State of the art". *Journal of Structural Engineering*. **133**(1): p. 57-66.

24 Bradley, B.A. (2010) "Site-specific and spatially distributed ground-motion prediction of acceleration spectrum intensity". *Bulletin of the Seismological Society of America*. **100**(2): p. 792-801.

25 Bradley, B.A., Cubrinovski, M., MacRae, G.A. and Dhakal, R.P. (2009) "Ground-motion prediction equation for SI based on spectral acceleration equations". *Bulletin of the Seismological Society of America*. **99**(1): p. 277-285.

26 Bradley, B.A. (2011) "Empirical equations for the prediction of displacement spectrum intensity and its correlation with other intensity measures". *Soil Dynamics and Earthquake Engineering*. **31**(8): p. 1182-1191.

27 Chiou, B., Darragh, R., Gregor, N., and Silva, W. (2008) "NGA project strong-motion database". *Earthquake Spectra*. **24**(1): p. 23-44.

28 ASCE/SEI7-10, "Minimum Design Loads for Buildings and Other Structures, ASCE/SEI 7-10. American Society of Civil Engineers, Reston, Virginia", 2010.

APPENDICES: TABULATED CHARACERSTICS OF THE SELECTED GROUND MOTIONS

Presented in this appendix is the NGA ID number [26] of the 20 ground motions and their corresponding amplitude scale factor, selected for the scenario rupture of the Alpine, Hope, and Porters Pass faults for Christchurch city (Table A1-A3), and Wellington, Wairarapa, and Ohariu faults for Wellington city (Table A4-A6). Also, subsets of 7 ground motions from these 20 motions are presented in Appendix B.

It is important to note that the ground-motion selection has been conducted based on the geometric mean of the intensity measures of motion. Presented ground-motion time series are the as-recorded motions in two horizontal directions and the vertical direction (which have file names with suffix "_1", "_2", and "_3" for the two horizontal and vertical components; accessible at https://sites.google.com/site/brendonabradley/research/ground-motion-selection). Geometric mean of peak ground acceleration (PGA) and peak ground velocity (PGV) of the two as-recorded horizontal motions are presented in the tables below. These motions are also accessible at http://peer.berkeley.edu/nga/, using the NGA ID number.

APPENDIX A: ENSAMBLES OF 20 GROUND MOTIONS

Table A1. Selected ground motions representing the Alpine fault scenario rupture for Christchurch city

NGA#	Event	Year	Station	M_w	Mechanism	R_{rup}(km)	V_{s30}(m/s)	PGA (g)	PGV (cm/s)	Scale factor
836	Landers	1992	Baker Fire Station	7.28	Strike-Slip	87.9	271.4	0.11	9.85	1.18
842	Landers	1992	Brea - S Flower Av	7.28	Strike-Slip	137.4	308.6	0.04	10.50	2.74
860	Landers	1992	Hemet Fire Station	7.28	Strike-Slip	68.7	338.5	0.09	5.60	0.74
869	Landers	1992	LA - N Westmoreland	7.28	Strike-Slip	159.1	315.1	0.04	3.55	4.41
888	Landers	1992	San Bernardino - E & Hospitality	7.28	Strike-Slip	79.8	271.4	0.08	17.16	0.68
895	Landers	1992	Tarzana - Cedar Hill	7.28	Strike-Slip	175.7	257.2	0.05	7.07	1.10
1188	Chi-Chi- Taiwan	1999	CHY016	7.62	Reverse-Oblique	66.7	200.9	0.10	16.14	0.88
1192	Chi-Chi- Taiwan	1999	CHY023	7.62	Reverse-Oblique	81.3	279.8	0.05	9.08	1.04
1217	Chi-Chi- Taiwan	1999	CHY060	7.62	Reverse-Oblique	68.9	228.9	0.05	14.82	0.88
1223	Chi-Chi- Taiwan	1999	CHY067	7.62	Reverse-Oblique	83.6	228	0.06	10.33	0.66
1342	Chi-Chi- Taiwan	1999	ILA055	7.62	Reverse-Oblique	90.3	266.8	0.07	25.00	0.85
1415	Chi-Chi- Taiwan	1999	TAP010	7.62	Reverse-Oblique	101.3	226.4	0.10	22.80	0.85
1599	Duzce- Turkey	1999	Ambarli	7.14	Strike-Slip	188.7	175	0.03	5.59	2.55
1790	Hector Mine	1999	Huntington Beach - Lake St	7.13	Strike-Slip	184	370.8	0.02	10.02	3.34
1814	Hector Mine	1999	Newhall - Fire Sta	7.13	Strike-Slip	198.1	269.1	0.02	4.63	2.87
1823	Hector Mine	1999	Salton City	7.13	Strike-Slip	123.2	324.5	0.05	7.93	2.56
1837	Hector Mine	1999	Valyermo Forest Fire Station	7.13	Strike-Slip	135.8	345.4	0.06	6.36	1.37
2109	Denali- Alaska	2002	Fairbanks - Ester Fire Station	7.9	Strike-Slip	139.8	274.5	0.05	4.00	1.12
2115	Denali- Alaska	2002	TAPS Pump Station #11	7.9	Strike-Slip	126.4	376.1	0.08	11.52	0.67
2116	Denali- Alaska	2002	TAPS Pump Station #12	7.9	Strike-Slip	164.7	338.6	0.04	4.39	1.05

Table A2. Selected ground motions representing the Hope fault scenario rupture for Christchurch city

NGA#	Event	Year	Station	M_w	Mechanism	R_{rup}(km)	V_{s30}(m/s)	PGA (g)	PGV (cm/s)	Scale factor
82	San Fernando	1971	Port Hueneme	6.61	Reverse	68.8	297.9	0.03	5.43	1.18
742	Loma Prieta	1989	Bear Valley #1- Fire Station	6.93	Reverse-Oblique	61.7	338.5	0.07	5.87	1.52
832	Landers	1992	Amboy	7.28	Strike-Slip	69.2	271.4	0.13	19.00	0.55
887	Landers	1992	Riverside Airport	7.28	Strike-Slip	96	370.8	0.04	3.05	2.70
1068	Northridge-01	1994	San Bernardino - Co Service Bldg - Freefield	6.69	Reverse	107.7	271.4	0.04	4.65	2.25
1147	Kocaeli- Turkey	1999	Ambarli	7.51	Strike-Slip	69.6	175	0.21	36.67	0.28
1220	Chi-Chi- Taiwan	1999	CHY063	7.62	Reverse-Oblique	72.2	246.9	0.06	8.56	0.94
1332	Chi-Chi- Taiwan	1999	ILA042	7.62	Reverse-Oblique	85.7	209.4	0.08	16.67	0.75
1344	Chi-Chi- Taiwan	1999	ILA059	7.62	Reverse-Oblique	86.3	236.8	0.07	15.39	0.33
1433	Chi-Chi- Taiwan	1999	TAP047	7.62	Reverse-Oblique	84.5	400.3	0.06	15.20	1.28
1559	Chi-Chi- Taiwan	1999	TTN003	7.62	Reverse-Oblique	95	262.6	0.02	3.10	2.11
1766	Hector Mine	1999	Baker Fire Station	7.13	Strike-Slip	64.8	271.4	0.11	8.44	0.52
1773	Hector Mine	1999	Cabazon	7.13	Strike-Slip	76.9	345.4	0.04	7.40	0.80
1783	Hector Mine	1999	Fort Irwin	7.13	Strike-Slip	65.9	345.4	0.13	10.06	0.53
1813	Hector Mine	1999	Morongo Valley	7.13	Strike-Slip	53.2	345.4	0.08	16.52	1.94
1821	Hector Mine	1999	Pomona - 4th & Locust FF	7.13	Strike-Slip	143.4	229.8	0.04	6.42	0.60
1822	Hector Mine	1999	Riverside Airport	7.13	Strike-Slip	123.8	370.8	0.02	2.96	1.59
1823	Hector Mine	1999	Salton City	7.13	Strike-Slip	123.2	324.5	0.05	7.93	1.74
2089	Nenana Mountain- Alaska	2002	Fairbanks - Ester Fire Station	6.7	Strike-Slip	146.3	274.5	0.02	1.69	1.59
2115	Denali- Alaska	2002	TAPS Pump Station #11	7.9	Strike-Slip	126.4	376.1	0.08	11.52	0.59

Table A3. Selected ground motions representing the Porters Pass fault scenario rupture for Christchurch city

NGA#	Event	Year	Station	M_w	Mechanism	R_{rup}(km)	V_{s30}(m/s)	PGA (g)	PGV (cm/s)	Scale factor
51	San Fernando	1971	2516 Via Tejon PV	6.61	Reverse	55.2	280.6	0.03	3.43	1.67
93	San Fernando	1971	Whittier Narrows Dam	6.61	Reverse	39.5	298.7	0.12	9.30	2.02
176	Imperial Valley-06	1979	El Centro Array #13	6.53	Strike-Slip	22	249.9	0.13	14.23	2.71
190	Imperial Valley-06	1979	Superstition Mtn Camera	6.53	Strike-Slip	24.6	362.4	0.14	6.79	0.82
191	Imperial Valley-06	1979	Victoria	6.53	Strike-Slip	31.9	274.5	0.13	7.79	1.66
287	Irpinia- Italy-01	1980	Bovino	6.9	Normal	46.2	274.5	0.04	2.69	5.96
729	Superstition Hills-02	1987	Wildlife Liquef. Array	6.54	Strike-Slip	23.9	207.5	0.20	27.82	0.66
761	Loma Prieta	1989	Fremont - Emerson Court	6.93	Reverse-Oblique	39.9	284.8	0.16	13.57	0.79
762	Loma Prieta	1989	Fremont - Mission San Jose	6.93	Reverse-Oblique	39.5	367.6	0.14	11.36	1.01
850	Landers	1992	Desert Hot Springs	7.28	Strike-Slip	21.8	345.4	0.16	20.42	2.55
880	Landers	1992	Mission Creek Fault	7.28	Strike-Slip	27	345.4	0.12	12.63	1.00
900	Landers	1992	Yermo Fire Station	7.28	Strike-Slip	23.6	353.6	0.22	36.40	0.83
1026	Northridge-01	1994	Lawndale - Osage Ave	6.69	Reverse	39.9	361.2	0.12	8.25	1.09
1059	Northridge-01	1994	Port Hueneme - Naval Lab.	6.69	Reverse	51.8	271.4	0.09	8.09	2.70
1215	Chi-Chi- Taiwan	1999	CHY058	7.62	Reverse-Oblique	59.8	237.6	0.06	12.11	1.67
1228	Chi-Chi- Taiwan	1999	CHY076	7.62	Reverse-Oblique	42.2	169.8	0.08	19.56	0.60
1258	Chi-Chi- Taiwan	1999	HWA005	7.62	Reverse-Oblique	47.6	489.2	0.14	14.34	0.81
1279	Chi-Chi- Taiwan	1999	HWA030	7.62	Reverse-Oblique	47	487.4	0.07	12.25	1.63
1762	Hector Mine	1999	Amboy	7.13	Strike-Slip	43	271.4	0.20	23.90	1.42
1776	Hector Mine	1999	Desert Hot Springs	7.13	Strike-Slip	56.4	345.4	0.07	8.83	2.56

Table A4. Selected ground motions representing the Wellington fault scenario rupture for Wellington city

NGA#	Event	Year	Station	M_w	Mechanism	R_{rup}(km)	V_{s30}(m/s)	PGA (g)	PGV (cm/s)	Scale factor
161	Imperial Valley-06	1979	Brawley Airport	6.53	Strike-Slip	10.4	208.7	0.18	35.97	3.70
173	Imperial Valley-06	1979	El Centro Array #10	6.53	Strike-Slip	6.2	202.8	0.20	42.95	4.40
175	Imperial Valley-06	1979	El Centro Array #12	6.53	Strike-Slip	17.9	196.9	0.13	19.64	3.09
179	Imperial Valley-06	1979	El Centro Array #4	6.53	Strike-Slip	7	208.9	0.41	55.89	1.74
183	Imperial Valley-06	1979	El Centro Array #8	6.53	Strike-Slip	3.9	206.1	0.53	50.23	1.35
723	Superstition Hills-02	1987	Parachute Test Site	6.54	Strike-Slip	0.9	348.7	0.38	72.74	2.64
729	Superstition Hills-02	1987	Wildlife Liquef. Array	6.54	Strike-Slip	23.9	207.5	0.20	27.82	1.55
776	Loma Prieta	1989	Hollister - South & Pine	6.93	Reverse-Oblique	27.9	370.8	0.29	48.34	2.71
806	Loma Prieta	1989	Sunnyvale - Colton Ave.	6.93	Reverse-Oblique	24.2	267.7	0.20	34.42	1.86
880	Landers	1992	Mission Creek Fault	7.28	Strike-Slip	27	345.4	0.12	12.63	2.73
900	Landers	1992	Yermo Fire Station	7.28	Strike-Slip	23.6	353.6	0.22	36.40	2.82
1084	Northridge-01	1994	Sylmar - Converter Sta	6.69	Reverse	5.3	251.2	0.69	110.25	1.73
1176	Kocaeli- Turkey	1999	Yarimca	7.51	Strike-Slip	4.8	297	0.29	59.27	2.40
1194	Chi-Chi- Taiwan	1999	CHY025	7.62	Reverse-Oblique	19.1	277.5	0.16	42.59	3.57
1244	Chi-Chi- Taiwan	1999	CHY101	7.62	Reverse-Oblique	10	258.9	0.41	96.39	1.38
1499	Chi-Chi- Taiwan	1999	TCU060	7.62	Reverse-Oblique	8.5	495.8	0.15	39.86	2.28
1503	Chi-Chi- Taiwan	1999	TCU065	7.62	Reverse-Oblique	0.6	305.9	0.69	101.37	1.83
1528	Chi-Chi- Taiwan	1999	TCU101	7.62	Reverse-Oblique	2.1	504.4	0.23	60.18	1.12
1547	Chi-Chi- Taiwan	1999	TCU123	7.62	Reverse-Oblique	14.9	241.7	0.15	39.01	1.58
2114	Denali- Alaska	2002	TAPS Pump Station #10	7.9	Strike-Slip	2.7	329.4	0.30	107.63	1.41

Table A5. Selected ground motions representing the Wairarapa fault scenario rupture for Wellington city

NGA#	Event	Year	Station	M_w	Mechanism	R_{rup}(km)	V_{s30}(m/s)	PGA (g)	PGV (cm/s)	Scale factor
850	Landers	1992	Desert Hot Springs	7.28	Strike-Slip	21.8	345.4	0.16	20.42	1.84
864	Landers	1992	Joshua Tree	7.28	Strike-Slip	11	379.3	0.28	34.15	3.28
880	Landers	1992	Mission Creek Fault	7.28	Strike-Slip	27	345.4	0.12	12.63	3.07
881	Landers	1992	Morongo Valley	7.28	Strike-Slip	17.3	345.4	0.16	18.15	4.34
882	Landers	1992	North Palm Springs	7.28	Strike-Slip	26.8	345.4	0.13	12.76	4.15
900	Landers	1992	Yermo Fire Station	7.28	Strike-Slip	23.6	353.6	0.22	36.40	2.62
1158	Kocaeli- Turkey	1999	Duzce	7.51	Strike-Slip	15.4	276	0.33	52.60	1.09
1194	Chi-Chi- Taiwan	1999	CHY025	7.62	Reverse-Oblique	19.1	277.5	0.16	42.59	2.49
1201	Chi-Chi- Taiwan	1999	CHY034	7.62	Reverse-Oblique	14.8	378.8	0.31	38.37	2.94
1203	Chi-Chi- Taiwan	1999	CHY036	7.62	Reverse-Oblique	16.1	233.1	0.26	38.07	2.73
1209	Chi-Chi- Taiwan	1999	CHY047	7.62	Reverse-Oblique	24.1	291.9	0.18	21.27	1.59
1244	Chi-Chi- Taiwan	1999	CHY101	7.62	Reverse-Oblique	10	258.9	0.41	96.39	2.18
1484	Chi-Chi- Taiwan	1999	TCU042	7.62	Reverse-Oblique	26.3	424	0.20	43.68	2.33
1491	Chi-Chi- Taiwan	1999	TCU051	7.62	Reverse-Oblique	7.7	467.5	0.19	43.65	1.74
1495	Chi-Chi- Taiwan	1999	TCU055	7.62	Reverse-Oblique	6.4	447.8	0.22	39.03	1.38
1499	Chi-Chi- Taiwan	1999	TCU060	7.62	Reverse-Oblique	8.5	495.8	0.15	39.86	2.99
1503	Chi-Chi- Taiwan	1999	TCU065	7.62	Reverse-Oblique	0.6	305.9	0.69	101.37	1.58
1513	Chi-Chi- Taiwan	1999	TCU079	7.62	Reverse-Oblique	11	364	0.54	54.50	1.80
1528	Chi-Chi- Taiwan	1999	TCU101	7.62	Reverse-Oblique	2.1	504.4	0.23	60.18	2.10
1553	Chi-Chi- Taiwan	1999	TCU141	7.62	Reverse-Oblique	24.2	209.2	0.09	35.36	2.62

Table A6. Selected ground motions representing the Ohariu fault scenario rupture for Wellington city

NGA#	Event	Year	Station	M_w	Mechanism	R_{rup}(km)	V_{s30}(m/s)	PGA (g)	PGV (cm/s)	Scale factor
162	Imperial Valley-06	1979	Calexico Fire Station	6.53	Strike-Slip	10.4	231.2	0.24	18.47	2.16
165	Imperial Valley-06	1979	Chihuahua	6.53	Strike-Slip	7.3	274.5	0.27	28.65	1.73
169	Imperial Valley-06	1979	Delta	6.53	Strike-Slip	22	274.5	0.28	27.01	1.22
172	Imperial Valley-06	1979	El Centro Array #1	6.53	Strike-Slip	21.7	237.3	0.14	12.97	3.62
176	Imperial Valley-06	1979	El Centro Array #13	6.53	Strike-Slip	22	249.9	0.13	14.23	5.07
187	Imperial Valley-06	1979	Parachute Test Site	6.53	Strike-Slip	12.7	348.7	0.16	16.06	1.61
192	Imperial Valley-06	1979	Westmorland Fire Sta	6.53	Strike-Slip	15.2	193.7	0.09	15.54	4.09
721	Superstition Hills-02	1987	El Centro Imp. Co. Cent	6.54	Strike-Slip	18.2	192.1	0.26	43.30	1.41
725	Superstition Hills-02	1987	Poe Road (temp)	6.54	Strike-Slip	11.2	207.5	0.34	29.46	2.01
728	Superstition Hills-02	1987	Westmorland Fire Sta	6.54	Strike-Slip	13	193.7	0.22	28.62	3.12
776	Loma Prieta	1989	Hollister - South & Pine	6.93	Reverse-Oblique	27.9	370.8	0.29	48.34	1.51
778	Loma Prieta	1989	Hollister Diff. Array	6.93	Reverse-Oblique	24.8	215.5	0.29	42.56	1.53
803	Loma Prieta	1989	Saratoga - W Valley Coll.	6.93	Reverse-Oblique	9.3	370.8	0.32	65.43	3.95
900	Landers	1992	Yermo Fire Station	7.28	Strike-Slip	23.6	353.6	0.22	36.40	2.43
1176	Kocaeli- Turkey	1999	Yarimca	7.51	Strike-Slip	4.8	297	0.29	59.27	1.35
1244	Chi-Chi- Taiwan	1999	CHY101	7.62	Reverse-Oblique	10	258.9	0.41	96.39	1.65
1499	Chi-Chi- Taiwan	1999	TCU060	7.62	Reverse-Oblique	8.5	495.8	0.15	39.86	2.72
1502	Chi-Chi- Taiwan	1999	TCU064	7.62	Reverse-Oblique	16.6	357.5	0.11	43.94	2.45
1537	Chi-Chi- Taiwan	1999	TCU111	7.62	Reverse-Oblique	22.1	237.5	0.12	45.32	4.12
2114	Denali- Alaska	2002	TAPS Pump Station #10	7.9	Strike-Slip	2.7	329.4	0.30	107.63	0.88

APPENDIX B: ENSAMBLES OF 7 GROUND MOTIONS

A subset of 7 ground motions from the selected 20 motions representing the scenario rupture of the Alpine, Hope, and Porters Pass faults for Christchurch city (Table B1-B3) and Wellington, Wairarapa, and Ohariu faults for Wellington city (Table B4-B6).

Table B1. Selected ground motions representing the Alpine fault scenario rupture for Christchurch city

NGA#	Event	Year	Station	M_w	Mechanism	R_{rup}(km)	V_{s30}(m/s)	PGA (g)	PGV (cm/s)	Scale factor
888	Landers	1992	San Bernardino - E & Hospitality	7.28	Strike-Slip	79.8	271.4	0.08	17.16	1.07
895	Landers	1992	Tarzana - Cedar Hill	7.28	Strike-Slip	175.7	257.2	0.05	7.07	1.97
1188	Chi-Chi- Taiwan	1999	CHY016	7.62	Reverse-Oblique	66.7	200.9	0.10	16.14	0.87
1223	Chi-Chi- Taiwan	1999	CHY067	7.62	Reverse-Oblique	83.6	228	0.06	10.33	0.88
1823	Hector Mine	1999	Salton City	7.13	Strike-Slip	123.2	324.5	0.05	7.93	0.61
2109	Denali- Alaska	2002	Fairbanks - Ester Fire Station	7.9	Strike-Slip	139.8	274.5	0.05	4.00	1.56
2115	Denali- Alaska	2002	TAPS Pump Station #11	7.9	Strike-Slip	126.4	376.1	0.08	11.52	0.90

Table B2. Selected ground motions representing the Hope fault scenario rupture for Christchurch city

NGA#	Event	Year	Station	M_w	Mechanism	R_{rup}(km)	V_{s30}(m/s)	PGA (g)	PGV (cm/s)	Scale factor
887	Landers	1992	Riverside Airport	7.28	Strike-Slip	96	370.8	0.04	3.05	1.40
1147	Kocaeli- Turkey	1999	Ambarli	7.51	Strike-Slip	69.6	175	0.21	36.67	0.29
1332	Chi-Chi- Taiwan	1999	ILA042	7.62	Reverse-Oblique	85.7	209.4	0.08	16.67	0.95
1344	Chi-Chi- Taiwan	1999	ILA059	7.62	Reverse-Oblique	86.3	236.8	0.07	15.39	0.43
1766	Hector Mine	1999	Baker Fire Station	7.13	Strike-Slip	64.8	271.4	0.11	8.44	0.82
1813	Hector Mine	1999	Morongo Valley	7.13	Strike-Slip	53.2	345.4	0.08	16.52	0.55
1823	Hector Mine	1999	Salton City	7.13	Strike-Slip	123.2	324.5	0.05	7.93	1.59

Table B3. Selected ground motions representing the Porters Pass fault scenario rupture for Christchurch city

NGA#	Event	Year	Station	M_w	Mechanism	R_{rup}(km)	V_{s30}(m/s)	PGA (g)	PGV (cm/s)	Scale factor
93	San Fernando	1971	Whittier Narrows Dam	6.61	Reverse	39.5	298.7	0.12	9.30	0.94
729	Superstition Hills-02	1987	Wildlife Liquef. Array	6.54	Strike-Slip	23.9	207.5	0.20	27.82	0.46
761	Loma Prieta	1989	Fremont - Emerson Court	6.93	Reverse-Oblique	39.9	284.8	0.16	13.57	1.31
762	Loma Prieta	1989	Fremont - Mission San Jose	6.93	Reverse-Oblique	39.5	367.6	0.14	11.36	2.37
880	Landers	1992	Mission Creek Fault	7.28	Strike-Slip	27	345.4	0.12	12.63	1.50
1026	Northridge-01	1994	Lawndale - Osage Ave	6.69	Reverse	39.9	361.2	0.12	8.25	0.57
1228	Chi-Chi- Taiwan	1999	CHY076	7.62	Reverse-Oblique	42.2	169.8	0.08	19.56	0.74

Table B4. Selected ground motions representing the Wellington fault scenario rupture for Wellington city

NGA#	Event	Year	Station	M_w	Mechanism	R_{rup}(km)	V_{s30}(m/s)	PGA (g)	PGV (cm/s)	Scale factor
173	Imperial Valley-06	1979	El Centro Array #10	6.53	Strike-Slip	6.2	202.8	0.20	42.95	3.17
175	Imperial Valley-06	1979	El Centro Array #12	6.53	Strike-Slip	17.9	196.9	0.13	19.64	1.96
729	Superstition Hills-02	1987	Wildlife Liquef. Array	6.54	Strike-Slip	23.9	207.5	0.20	27.82	2.24
806	Loma Prieta	1989	Sunnyvale - Colton Ave.	6.93	Reverse-Oblique	24.2	267.7	0.20	34.42	3.62
880	Landers	1992	Mission Creek Fault	7.28	Strike-Slip	27	345.4	0.12	12.63	4.71
1176	Kocaeli- Turkey	1999	Yarimca	7.51	Strike-Slip	4.8	297	0.29	59.27	2.33
1194	Chi-Chi- Taiwan	1999	CHY025	7.62	Reverse-Oblique	19.1	277.5	0.16	42.59	2.13

Table B5. Selected ground motions representing the Wairarapa fault scenario rupture for Wellington city

NGA#	Event	Year	Station	M_w	Mechanism	R_{rup}(km)	V_{s30}(m/s)	PGA (g)	PGV (cm/s)	Scale factor
850	Landers	1992	Desert Hot Springs	7.28	Strike-Slip	21.8	345.4	0.16	20.42	4.69
880	Landers	1992	Mission Creek Fault	7.28	Strike-Slip	27	345.4	0.12	12.63	5.41
882	Landers	1992	North Palm Springs	7.28	Strike-Slip	26.8	345.4	0.13	12.76	3.21
900	Landers	1992	Yermo Fire Station	7.28	Strike-Slip	23.6	353.6	0.22	36.40	3.97
1495	Chi-Chi- Taiwan	1999	TCU055	7.62	Reverse-Oblique	6.4	447.8	0.22	39.03	1.25
1503	Chi-Chi- Taiwan	1999	TCU065	7.62	Reverse-Oblique	0.6	305.9	0.69	101.37	0.58
1513	Chi-Chi- Taiwan	1999	TCU079	7.62	Reverse-Oblique	11	364	0.54	54.50	0.77

Table B6. Selected ground motions representing the Ohariu fault scenario rupture for Wellington city

NGA#	Event	Year	Station	M_w	Mechanism	R_{rup}(km)	V_{s30}(m/s)	PGA (g)	PGV (cm/s)	Scale factor
172	Imperial Valley-06	1979	El Centro Array #1	6.53	Strike-Slip	21.7	237.3	0.14	12.97	2.16
176	Imperial Valley-06	1979	El Centro Array #13	6.53	Strike-Slip	22	249.9	0.13	14.23	3.49
187	Imperial Valley-06	1979	Parachute Test Site	6.53	Strike-Slip	12.7	348.7	0.16	16.06	5.01
776	Loma Prieta	1989	Hollister - South & Pine	6.93	Reverse-Oblique	27.9	370.8	0.29	48.34	3.25
778	Loma Prieta	1989	Hollister Diff. Array	6.93	Reverse-Oblique	24.8	215.5	0.29	42.56	1.63
1244	Chi-Chi- Taiwan	1999	CHY101	7.62	Reverse-Oblique	10	258.9	0.41	96.39	1.18
1537	Chi-Chi- Taiwan	1999	TCU111	7.62	Reverse-Oblique	22.1	237.5	0.12	45.32	2.36